CEAS Space Journal (2024) 16:319–332
https://doi.org/10.1007/s12567-023-00498-9

ORIGINAL PAPER

Mission design for point-to-point passenger transport with reusable launch vehicles

Jascha Wilken[1] · **Steffen Callsen**[1]

Received: 6 January 2023 / Revised: 31 March 2023 / Accepted: 21 April 2023 / Published online: 6 May 2023

Abstract

With the progress of SpaceX's Starship system, a fully reusable launch system appears possible in the near future. With this technological advance, a new class of transport missions could become economically feasible: Rocket-propelled transport of passengers and cargo at near-orbital speeds from one point on the Earth to another. This mission type is investigated for two reference vehicles: Starship from SpaceX and the SpaceLiner concept, developed by DLR-SART. For both vehicles, the properties during reentry are assessed and the impact on the descent trajectory is investigated, including parametric studies with regard to the effect of launch heading and crossrange capability. While the SpaceLiner upper stage relies on its high hypersonic L/D to cover the majority of the distance in quasi-stationary flight within the atmosphere, the Starship relies mostly on a ballistic flight path at higher altitudes. The flight within the upper layers of the atmosphere allows the SpaceLiner to change its heading mid-flight through banking maneuvers and thus efficiently curve around populated areas. However, this prolonged flight at high velocities within the upper atmosphere does necessitate active cooling of the leading edges. An exemplary mission from Shanghai to California is optimized for both reference vehicles, with the optimization target being minimal peak heat loads. Due to the Starship's reliance on the ballistic portion of its flight to cover range, the peak heat flux is substantially higher on westward missions, compared to the eastward return flight.

Keywords point-to-point mission design · hypersonic passenger transport · reusable launcher · trajectory optimization · hypersonic reentry

Abbreviations

AoA	Angle of Attack
DLR	German Aerospace Center
ECI	Earth-Centered Inertial
FFSC	Full-Flow Staged Combustion
IAC	In-Air-Capturing
ITS	Interplanetary Transport System
I_{sp}	Specific Impulse
L/D	Lift-to-Drag ratio
LEO	Low Earth Orbit
MECO	Main Engine Cut-Off
n_x	Axial load factor
n_z	Normal load factor
PTP	Point-To-Point
RRC	Reference Reentry Conditions
RTLS	Return To Launch Site
SART	Space Launcher System Analysis department
SECO	Second stage Engine Cut-Off
SLB	SpaceLiner Booster
SLC	SpaceLiner Capsule
SLME	SpaceLiner Main Engine
SLO	SpaceLiner Orbiter

✉ Jascha Wilken
jascha.wilken@dlr.de

[1] Deutsches Zentrum für Luft- und Raumfahrt, Institut für Raumfahrtsysteme, Robert-Hooke-Straße 7, 28359 Bremen, Germany

1 Introduction

With the first orbital flight test of SpaceX's Starship [1] coming closer, for the first time in human history, a fully reusable orbital transportation system might become operational. If SpaceX achieves its goal of quickly and economically reusing these vehicle stages, it is expected to substantially reduce the cost of transporting payloads to Low Earth Orbit (LEO) and significantly disrupt the orbital transport market.

This cost reduction might also lead to economic feasibility of an entirely new market: High-speed point-to-point (PTP) transport of cargo and humans. Essentially, flying at

near-orbital speed promises the ability to travel between two points on Earth in less than 60 min. This mission type has been previously discussed by SpaceX [2]; however, no detailed information on the specific mission scenario is publicly available.

The DLR-SART concept SpaceLiner, first proposed in 2005 [3], has been designed from conception for ultra-long-haul passenger transport. For both vehicles, the principal idea is to capture some share of the market between distant economical hubs for passenger or cargo that are willing to pay the higher prices for an order of magnitude reduction of travel time between the spaceports.

This paper compares the two very different and yet in some aspects surprisingly similar configurations and their PTP mission profiles and capabilities. The two configurations are described in section 2 and an initial comparison of their high-level properties is given in section 2.3. In chapter 3, the characteristics of both upper stages during reentry are evaluated and illustrated with reference reentry simulations as well as parametric variations of significant parameters. Finally, chapter 4 looks at the entire PTP mission and the differences between the two systems for a specific mission are evaluated.

2 Reference systems

This study focuses on evaluating PTP missions for two fully reusable rocket-propelled transportation systems. Both systems are also able to perform orbital missions, those are evaluated and discussed in other publications ([4] for SpaceLiner and [5] for Starship).In both cases, the aerodynamic properties discussed in this section and used in the following trajectory analysis include deflections of the control surfaces that achieve pitch trim.

2.1 SpaceX Starship

Since its presentation in 2016 [6], SpaceX's next-generation space transportation system has gone through multiple names and design iterations, but some key design features remained constant: Full reusability, Full-Flow Staged Combustion (FFSC) cycle engines and deeply subcooled LOX/LCH4 as propellants. Other features have been changed: While the initial Interplanetary Transport System (ITS) was supposed to weigh over 10,000 tons [6], the current design is projected to weigh about half of that. The main structure material was also changed from carbon fiber composites to stainless steel. The aerodynamic configurations of both stages have also been adapted and refined throughout the six years since the initial public presentation. An interim version, the BFR, has also been previously analyzed by DLR-SART [7].

The current iteration, dubbed Starship and Super Heavy [1], is the first where significant progress with regard to hardware integration of entire stages has been achieved. It is certain that the design will be further adapted and refined based on data from the first orbital tests. However, the current design is set to be the first fully integrated version that will attempt to reach orbit.

A description of the models used for the SpaceX's Starship including the descent of the reusable stages is given in [5] as well as an analysis of potential orbital transport missions. This data is based on DLR reverse engineering from publicly available data.

One aspect of Starship's design is of special interest for PTP missions: the reentry maneuver dubbed "Skydive". The reentry is done in three phases: First, the hypersonic deceleration at 70° angle of attack (AoA), followed by the skydive itself, during which the vehicle flies at close to 90° AoA, essentially maximizing the drag. This minimizes the terminal velocity and the propellant needed for the landing burn. The landing burn is the final phase of the Starship reentry, it includes a significant reorientation of the stage from 90° AoA to close to 180°.

The first stage of the Starship system is to be returned with a more classical approach, a similar Return To Launch Site (RTLS) scheme as used for the Falcon 9.

The Starship system's primary goal and ultimate design target is the transport of enough passengers and cargo to Mars to allow the construction of a self-sufficient human colony [6]. Thus, the chosen landing approach has to work in multiple atmospheric conditions, the relatively dense atmosphere of Earth as well as the thin atmosphere of Mars. Commercial missions such as the launch of Starlink satellites or PTP missions can be considered secondary missions. Their primary motivation is the generation of funding for the principal endeavor.

As reference payload of the PTP missions the mass given for the LEO missions was used (100t) [1].

2.2 SpaceLiner 7

Originally proposed in 2005 [3], the SpaceLiner concept has also gone through many design iterations, with the current development status shown in [8]. Since the initial conception, the reference mission for this concept has been the transport of passengers over extremely long distances at hypersonic speeds.

The current configuration SpaceLiner 7 (SL7) consists of the first stage SpaceLiner Booster (SLB) and the upper stage SpaceLiner Orbiter (SLO). A sketch of the configuration is shown in Fig. 1. The passengers are transported within the SpaceLiner Cabin (SLC), which can be detached from the SLO in the case of an emergency and is equipped to be able to safely reenter the atmosphere and land in water or on land.

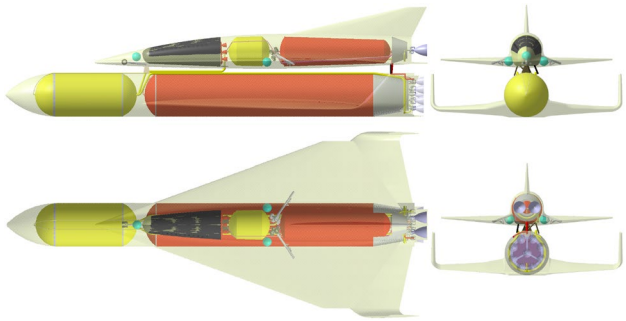

Fig. 1 Sketch of SpaceLiner 7 configuration, from [8]

Both stages are powered by the SpaceLiner Main Engine (SLME) which runs on a full-flow staged combustion cycle with liquid hydrogen and liquid oxygen as propellants. The booster stage has nine engines, while the passenger stage contains two. As all engines are active from lift-off until MECO, the engine is designed to work from sea level to vacuum conditions. A propellant cross-feed from the booster to the passenger stage is foreseen to reduce the overall size of the configuration.

The first stage, the SLB, is equipped with wings in order to do a horizontal reentry with AoA close to 45°. For the return to launch site, the In-Air-Capturing (IAC) method is used. After reentry, the SLB rendezvouses with a conventional aircraft and after a capturing maneuver is towed back to the launch site where it can land on a conventional runway. A detailed description of this method is given in [9].

The upper stage SLO is designed for a high lift/drag ratio (L/D) in the hypersonic regime, and can achieve a trimmed L/D of 3.5 at Mach 14, assuming a fully turbulent boundary layer. The prolonged flight within the atmosphere necessitates the use of an active cooling system at the leading edges [10], however it allows the SLO to cover significant downrange with comparatively low speed at Second stage Engine Cut-Off (SECO), as shown in section 3.2.

The SLO also has an alternative version for orbital satellite deliveries. The volume of the passenger capsule is replaced with the payload and an additional kick-stage for deliveries into high energetic orbits such as a GTO. The two-stage-to-orbit performance to a low Earth orbit without the kick-stage is approximately 26 tons. Using the kick-stage, it can deliver about 8.3 tons to a GTO while landing the orbiter at the launch site after a complete revolution around Earth [4].

2.3 Comparison

A DLR-SART analysis on previous Starship iterations as well as an initial comparison to the SpaceLiner system has been published previously [7]. Since then the Starship system design has undergone some significant changes and hardware refinements. Thus, a reiteration of this comparison is shown herein. Table 1 contains the key parameters for both launch systems.

Many differences in the vehicle's masses are caused by the different propellant combination: While the Starship uses subcooled LOX/LCH4 for both stages, the SL7 uses LOX/LH2. The significantly lower density of LH2 necessarily leads to higher structural indices due to the larger tank volume.

While both systems share the goal of full, rapid, and economical reuse, the methods chosen to recover each stage are different: Super Heavy and Starship rely on vertical landing, as well as being caught by movable arms on the launch tower [11]. Both stages of the SpaceLiner system rely on wings to decelerate sufficiently to perform a horizontal landing on a runway. The wings and associated subsystems, such as thermal protection system, add significant mass to the system and increase the structural index. This especially effects the upper stage, which has large wings in order to achieve a good hypersonic aerodynamic performance as well as non-integral tanks.

In comparison, the design choices of the Starship system, especially with regard to propellant and return method, lead to much lower structural indices and can thus compensate for the significantly lower specific impulse of the propellant combination LOX/LCH4.

With regard to payload, both vehicles have a similar payload ratio (1.8% for SL7 and 2% for Starship). They use different approaches to maintain a sufficiently high payload ratio, even in fully reusable mode: High I_{SP} vs. low structural index. It should be noted that the dry mass estimation for Starship does not account for structures needed to integrate its massive payload into the vehicle, nor for structural reinforcements necessary to allow for large openings/doors within the upper part of the Starship vehicle. No information is publicly available with regard to the interior design of Starship and it will likely vary significantly between different versions, depending on which mission shall be flown: PTP, LEO satellite transport, refueling, or missions to Moon or to Mars.

Both vehicles employ FFSC cycle engines. However, the target combustion chamber pressure for SpaceX's Raptor engine is almost twice the design value of the SLME.

With regard to the aerodynamic properties, the aerodynamic coefficients during reentry are the most relevant aspect for this analysis. During the hypersonic portion of the reentry, the AoA for the Starship is close to 70° and close to 12° for the SLO. While the amount of lift generated relative to the vehicle mass is to some extent larger for the SLO, the difference in the ballistic coefficient is almost an order of magnitude. The effects of these very different

Table 1 Key parameters of SpaceLiner 7 and Starship & Super Heavy (as of 2022)

	SpaceLiner 7	Starship and super heavy
1st stage		
Propellant mass	1272 t	3400 t
Dry mass	198 t	270 t
Structural index	15.6%	7.9%
Total mass	1467 t	3670 t
Engine I_{SP}, sea level	386 s	326 s
Engine I_{SP}, vacuum	439 s	349 s
Return method	IAC	RTLS
Length	82.3 m	70 m
Fuselage diameter	8.6 m	9 m
2nd stage		
Propellant mass	232 t	1200 t
Dry mass	95 t	130 t
Structural index	40.1%	10.6%
Total mass	342 t	1330 t
Engine I_{SP}, sea level	362 s	285 s
Engine I_{SP}, vacuum	451 s	374 s
Length	65.6 m	50 m
Fuselage diameter	6.4 m	9 m
Total mass	1843 t	4997 t
Reference payload	34 t	100 t
Reentry aerodynamics		
Reference reentry angle of attack	12°	70°
Hypersonic L/D for reference reentry conditions (RRC)	~3	~0.3
Ballistic coefficient for RRC	4000 kg/m^2	510 kg/m^2
Lifting ballistic coefficient for RRC, as defined in Eq. (2)	1300 kg/m^2	1700 kg/m^2
Crew Separation System	Passenger capsule	No information

aerodynamic configurations and approaches are further discussed in chapter 3.

Some of the differing design choices are also induced by the primary mission of the reference system: While the SpaceLiner's main focus is the PTP missions discussed herein, the primary goal of the Starship system is the transport of vast amounts of propellants to LEO in order to fuel a subset of the Starship fleet that shall journey to Mars. So, for example, the design driver of the reentry mode of the Starship is not the capability for long range hypersonic glide but rather the safe return from orbit with the minimum amount of inert mass and quick stage turnaround. Also, since Starship is envisioned to be able to land on Earth, Mars and the Moon, the system has to be able to land in the relevant ambient conditions. On the other hand, the high hypersonic L/D of the SLO is not strictly needed for orbital reentry after a LEO transport mission, but instead results from the shared shape with the PTP version.

In both cases, these vehicles are able to address multiple missions, but are optimized for one. The suboptimal version will still be able to benefit from the increased production rate and commonalities with the versions used for other missions.

Finally, it should be noted that even though Starship hardware is being built (at an impressive rate), neither system is operational or has reached the final design iteration as of today, so for future iterations, the comparison might well be very different.

3 Reentry

For all reusable launch vehicles, the main goal for the reentry from orbit is the same: Safe deceleration from orbital velocities without exceeding the permissible mechanical and thermal loads and subsequent landing within the designated area.

In order to reduce the heat fluxes to levels acceptable for the overall system design, the goal is to dissipate much of the energy in the upper layers of the atmosphere, only entering into the denser, lower layers of the atmosphere with reduced velocity. The simplest strategy to achieve this, is to use a design with a very low ballistic coefficient C_b. C_b is defined as the ratio of the reentry mass m to the drag coefficient C_d times the reference surface area A_{ref}.

$$C_b = \frac{m}{C_d \cdot A_{ref}} \quad (1)$$

With a low enough ballistic coefficient, the low density of the upper atmosphere is sufficient to decelerate the vehicle without generating excessive heat fluxes.

If the vehicle is able to generate a significant amount of lift, this enables a shallower reentry which can further reduce the peak heat flux. However, the normal (n_Z) loads induced by the lift during reentry can be a sizing factor for the vehicles structures and cannot be excessively large, especially for a crewed vehicle.

In order to compare the reentry behavior of both vehicles two parameters are used: First, the established ballistic coefficient and then additionally an equivalent coefficient with regard to lift, as defined below:

$$C_{b,l} = \frac{m}{C_l \cdot A_{ref}} \quad (2)$$

In essence, these coefficients describe to which degree the trajectory within the atmosphere is affected by generated lift or drag. The higher the value, the more "resistant" the vehicle is to changes from that source.

Surprisingly, the value of $C_{b,l}$ is actually in a similar range for both vehicles at their reference reentry angle of attack. Thus, for similar state conditions the two vehicles experience similar accelerations through lift. A larger difference is found in the ballistic coefficient C_b, the value of the SLO being almost an order of magnitude larger than of the Starship. This high ballistic coefficient, coupled with the high L/D ratio, is essentially what allows the SpaceLiner to engage in sustained high-velocity flight through the upper layers of the atmosphere. Assuming the same initial conditions, the Starship would decelerate much faster. This aids the Starship in avoiding excessive peak heat fluxes but limits the gliding range.

In contrast, due to the high ballistic coefficient, the SLO relies on the lift generation in order to remain at higher altitudes and avoid the high thermal loads that would ensue if the stage entered the denser parts of the atmosphere without significantly reducing its velocity first. For a standard reentry vehicle, this is not an optimal reentry strategy since it results in a long flight at significant heat flux. However, in contrast to the Starship or other conventional reentry capsules, the SLO is optimized to cover a large downrange distance while within the atmosphere. This prolonged flight within the atmosphere also allows the stage to change its heading through banking maneuvers and thus, to a certain degree, deviate from straight connections between two points on Earth. This is shown in the missions discussed in section 3.3.

In order to quantify and illustrate the aforementioned differences, a parametric study of the reentry of both vehicles was simulated with the following assumptions:

- Initial conditions:
  - 80 km altitude
  - 7.4 km/s relative velocity
  - 0° flight path angle
  - 90° heading
  - -180° longitude
  - 0° latitude
- Controls
  - Constant angle of attack
    a. 12° for SLO
    b. 70° for Starship
  - Varied bank angle between ±45°

The results are shown in the following figures. The accompanying comparisons and analysis are relevant for the atmospheric reentry, but cannot be transferred directly to the PTP mission. For a full mission, the ascent is also optimized with regard to the vehicle's descent properties, so the initial conditions of the reentry will differ. However, the insights discussed within this section do inform some of the properties of the full PTP missions shown in chapter 4.

As with the following full mission optimizations, the landing is not simulated since it has no impact on the loads during reentry. For the Starship, the appropriate amount of propellant required for landing (or decelerating and hovering next to the launch tower) is included in the mass budget as inert mass.

The flight path for both vehicles is shown in Fig. 2. For this and all following figures, the trajectory of the reentry with a bank angle of 0° is shown by the medium blue/orange

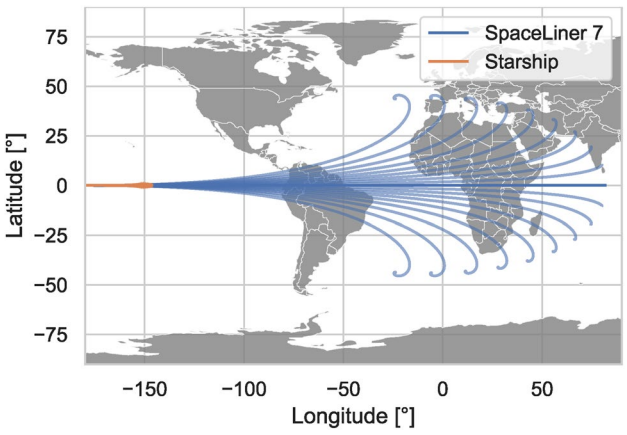

Fig. 2 Reentry path for Starship and SpaceLiner Orbiter with parametric variation of bank angle

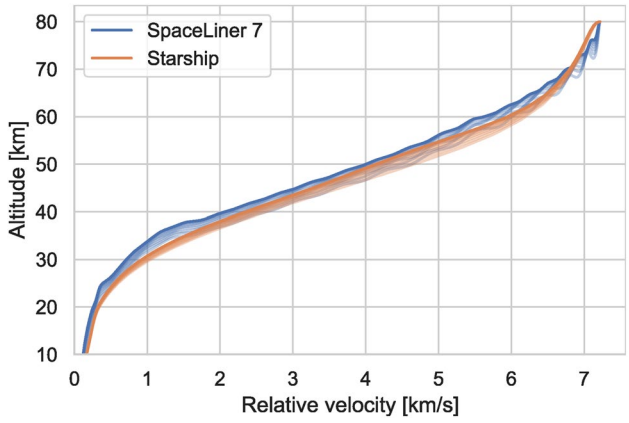

Fig. 3 Reentry profile for Starship and SpaceLiner Orbiter with parametric variation of bank angle

line, with all bank angle variations being drawn in lighter shades.

The difference between the two vehicles is clearly apparent: While the Starship does, in absolute terms, still cover a large distance (~3800 km), it is small in comparison to the distance covered by the SLO (~29,000 km). The cross-range achievable by the SLO is also much larger. From the initial starting point over the Pacific, the stage is able to reach Portugal, India, or South Africa. The true cross-range capability is even larger, since a constant bank angle is not optimal for the final portion of the flight. This can be seen in the flight paths, as they curl inwards near the end of the simulated trajectories. However, this simplified parametric study illustrates the differences for the reentry sufficiently well.

The reentry profiles resulting from this parametric study for both upper stages are shown in Fig. 3.

Even though both vehicles pursue very different reentry strategies, the reentry profile is similar. This is due to both stages being designed to avoid entering the denser parts of the atmosphere at high velocities. While the time scale is very different, both follow a similar descent path, the Starship quickly decelerating and descending and the SLO decelerating slowly but also staying at higher altitudes longer.

3.1 Loads during reentry

As mentioned above, both vehicles avoid flying at high velocities in the dense parts of the atmosphere and thus follow a similar reentry profile.

Within the following results, the heat flux is estimated for the stagnation point with a modified Chapman equation as shown in the following Eq. (3). Here, ρ is the local density at the respective altitude according to the US standard atmosphere 1976, ρ_R is a reference density value of 1.225 kg/m^3, $R_{N,r}$ is reference nose radius (here 1 m), R_N is the vehicle nose radius, v is the vehicle's velocity and v_R is a reference velocity of 10,000 m/s.

$$\dot{q} = 20254.4\mathrm{W/cm^2} \cdot \sqrt{\frac{\rho}{\rho_R}\frac{R_{N,r}}{R_N}}\left(\frac{v}{v_r}\right)^{3.05} \tag{3}$$

With this method, the selection of a useful nose radius is necessary. Since both vehicles have very different shapes, different values apply. In the previously given references for the SpaceLiner, the wing leading edge radius of 20.5 cm is used for R_N, while for the Starship, the fuselage radius of 4.5 m was used since at reentry the stage is almost perpendicular to the flow. Estimated with Eq. 3, this results in a ~4.7-fold higher maximum local heat flux at the same velocity and altitude for the leading wing edge of the SpaceLiner compared to the fuselage of the Starship. However, it is likely that the flaps or other protrusions of the Starship experience higher heat flux than its fuselage. In order to reliably assess the heat flux for the entire vehicle, CFD calculations would be necessary with the complete geometry, including any sharp edges or small protrusions.

In order to be able to compare the flow conditions encountered during the reentry, a nose radius of 20.5 cm is used within this section for both vehicles for estimation of the stagnation point heat flux.

The evolution of the heat flux over the entire trajectory is shown in Fig. 4. In both cases, similar peak heat fluxes are experienced, but with large differences with regard to the timeline, since Starships reentry is completed much quicker and the SpaceLiner maintains flight at high velocities within the atmosphere for over an hour. This is the reason why the SLO has to use active cooling in the leading edges of the wings.

The variation of bank angle appears to have a larger effect on the thermal loads of the SLO stage, noticeably increasing

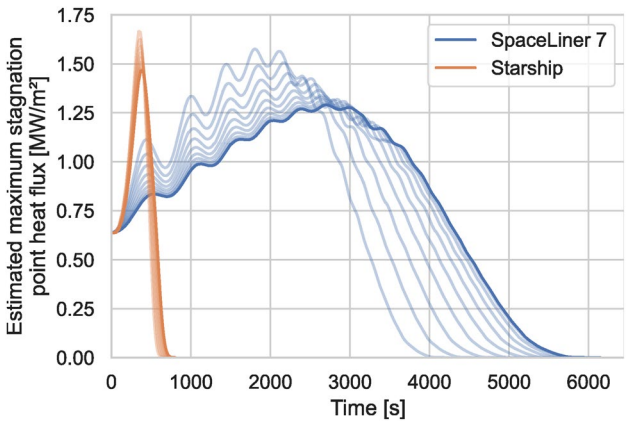

Fig. 4 Estimated stagnation point heat flux for Starship and SpaceLiner Orbiter for a nose radius of 20.5 cm with parametric variation of bank angle

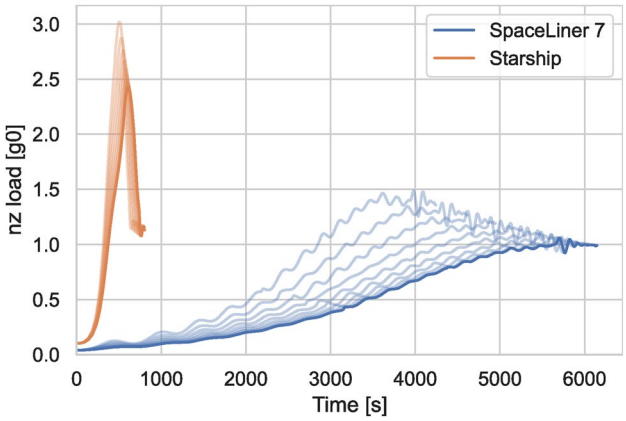

Fig. 5 Normal acceleration loads for Starship and SpaceLiner Orbiter with parametric variation of bank angle

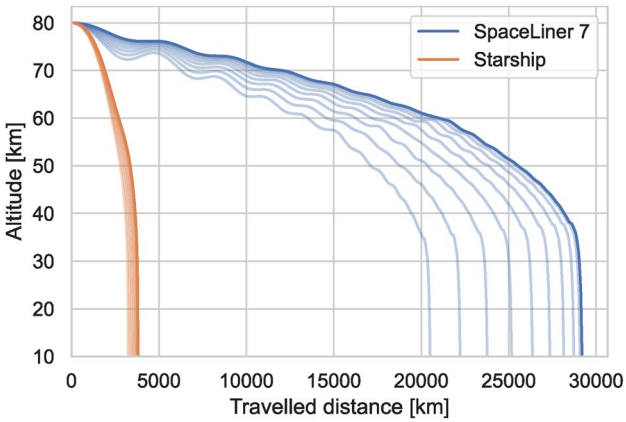

Fig. 6 Distance traveled for Starship and SpaceLiner Orbiter with parametric variation of bank angle

the peak heat flux. Since the bank angle changes the direction of the produced lift, the stage descends more rapidly into the atmosphere, which leads to higher heat fluxes. This also affects the Starship, but since it mostly relies on high drag to reduce the peak heat flux, the effect is smaller but still noticeable.

The n_Z loads experienced by the vehicles and their passengers are shown in Fig. 5. While the SLO slowly and continuously decelerates, the trajectory of Starship leads to a quicker deceleration with higher maximum loads.

It has to be noted that for both vehicles, the largest acceleration during ascent is along the vehicle axis (n_X) while the peak acceleration during descent is perpendicular to that (n_Z). This needs to be considered when positioning the passenger seats as the human tolerances for g-force depends on the direction of the acceleration and is lowest parallel to the spine.

3.2 Downrange capability

From the properties discussed above and the trajectories shown in Fig. 2, it is clear that, starting from the entry interface, the SLO can cover much more downrange distance than the Starship. The distance traveled is shown in Fig. 6.

This, of course, only applies to the atmospheric flight portion of the mission. Starship is capable of covering large distances in a ballistic arc, before entering the atmosphere. In contrast, the SLO has the added flexibility of being able to cover substantial amounts of distance both in quasi-stationary atmospheric flight as well as in ballistic phases before entering the atmosphere.

3.3 Cross-range capability

The variation of the bank angle allows a rough estimate of the cross-range capability, although for a truly maximal cross-range at a given downrange distance a variable bank angle would be optimal. However, this simplistic parametric study is sufficient to illustrate the large difference between the systems' capabilities. Due to the fact that the SLO spends a much longer time in the atmosphere, the change in bank angle has a significant effect (see Fig. 2).

In absolute terms however, the cross-range capability of the Starship is not small. Between the landing points for the cases with $\pm 45°$ bank angle, a ~ 300 km distance exists, effectively a 150 km cross-range. While still much smaller than for the SLO, this range can be used to correct errors in the SECO conditions in order to still land at the designated position.

This study only analyzed the possibility of achieving cross-range with aerodynamic means. In theory, a propulsive maneuver could be used to change the direction of the flight path. Depending on the level of change desired, this would necessitate a substantial Δv budget and might thus be undesirable from a performance perspective. In later analysis, this might be an option for shorter routes with low Δv requirements where a densely populated area could be avoided.

3.4 Effect of heading

While for orbital reentries, the heading is often eastward, for PTP systems, the heading depends on the targeted landing site and will vary from mission to mission.

In order to assess the effect of the heading on the reentry portion of the flight, the previously discussed parametric study is done for the same initial conditions with the following changes.

- Bank angles are kept at 0°
- 90° and -90° heading

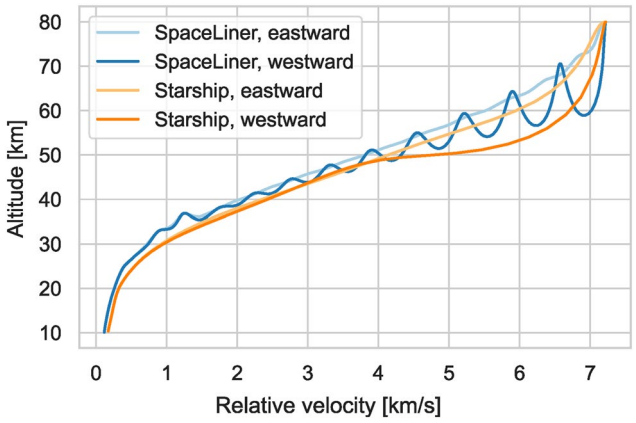

Fig. 7 Reentry profile for Starship and SpaceLiner Orbiter with east- and westward heading

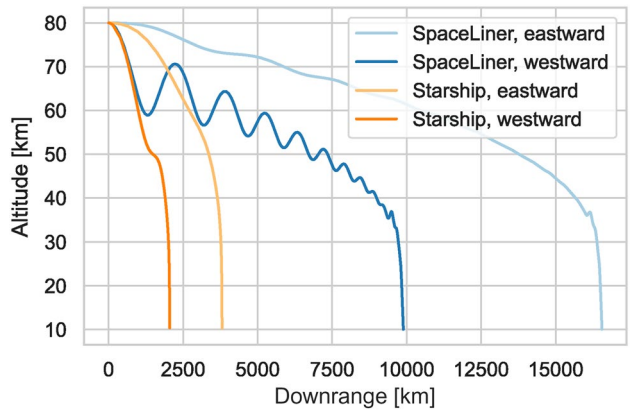

Fig. 8 Distance traveled for Starship and SpaceLiner Orbiter for east- and westward heading

The initial relative velocity is kept identical for both headings. While this does not reflect an orbital reentry, where the inertial velocity would initially be identical, this can be considered representative of a PTP trajectory. It is expected that a similar ascent of the same launcher toward the east and the west would lead to the same relative velocities, barring some minor differences in the losses experienced during the ascent.

The resulting trajectory is shown in the following figures. As can be seen in Fig. 7, both vehicles lose significantly more altitude at higher velocities when flying westward.

This not only affects the loads on the vehicle but significantly reduces the downrange capability, as can be seen in Fig. 8. Thus, for both vehicles, the distance traversed within the atmosphere is more limited when traveling westward, even if the initial relative velocity is identical.

This is essentially caused by the difference in inertial velocity. For the given initial conditions, the heading makes the difference between being on an 80 km x − 440 km orbit when flying east or an 80 km x− 2600 km orbit when flying west. This is due to the speed added or subtracted by the Earth's rotation. The far lower apogee results in a significantly steeper path into the atmosphere and thus a subsequent range loss.

From a vehicle-centric force balance perspective, this essentially means the centrifugal force experienced by the vehicle is significantly lower if its flying with the same relative velocity west rather than east due to the difference in inertial velocity.

However, the reentry is only the final portion of the mission, and the ascent and ballistic phases can potentially compensate the loss of range. The effect on the full mission is discussed in section 4.2.1.

4 P2P Mission design

The final step of this analysis is the evaluation of the entire mission delivering a payload, potentially including passengers, from one point on Earth to another.

The following section 4.1.2 describes how the mission was evaluated for Starship. The SpaceLiner was evaluated with similar methods that are described in detail in [12] and will be briefly summarized in section 4.1.1. First, the effect of launch heading is evaluated and discussed with another parametric study for a mission with a generic range requirement, presented in 4.2.1, and finally a specific PTP mission is presented and discussed in section 4.2.2.

4.1 Methods

4.1.1 SpaceLiner mission

The constraints and controls as well as the initial and final conditions used for the SpaceLiner trajectories have been discussed in [12]. Both ascent and descent trajectories are integrated with the given controls, and a global evolutionary optimization framework is used to identify an optimal solution that fulfills all constraints.

Noteworthy is the inclusion of population density within the overflown area as an additional optimization objective. This was not included for the Starship trajectory. While the vehicle does have some cross-range capability, it does not have the same flexibility in curving around populated areas as the SLO does.

4.1.2 Starship mission

As for the SpaceLiner, the entire Starship mission is optimized. Both ascent and descent are coupled, with the propellant needed for the return and landing of the first stage

estimated via the calculation of the ballistic arch necessary to arrive back at the launch pad. The propellant necessary for the final deceleration of the first stage depends on its terminal velocity, which is known from prior studies [5].

The combined ascent and descent trajectories are then evaluated with regard to their adherence to the constraints and the performance with regard to the optimization objective(s).

4.1.2.1 Constraints The main constraints set for the trajectory of the Starship concern the maximum mechanical loads. A maximum n_Z acceleration of 2.5 g was set as constraint, so that the loads remain similar to the loads encountered during orbital reentry [5]. Additionally, a maximum permissible dynamic pressure of 60 kPa was set as a constraint. Since the peak heat flux was the optimization objective, its value was not constrained for the Starship mission simulations. Finally, the deviation from the target coordinates was constrained as well as the final altitude, in order to make sure that the result found by the optimizer actually intersects with Earth's surface. Since the skydive decouples the orbital reentry from the final landing maneuver, the landing was not simulated, but the necessary propellant was included as inert mass in the mass models. Thus, the trajectory was not evaluated below 10 km altitude and no further constraints with regard to e.g., vehicle orientation during landing were considered.

4.1.2.2 Controls Theoretically, these missions have an extremely large number of possible control parameters, especially for controls such as the AoA which can be discretized for any number of time points. Due to computational constraints, it is desirable to reduce the number of controls, since each additional control parameter represents an additional degree of freedom that has to be explored. However, using too few controls might unintentionally constrain the problem and limit it from finding optimal solutions. For the optimizations of the Starship system presented in the subsequent sections, the following controls were used:

- Second stage burn time
- Launch azimuth
- Pitching rate (at initiation of gravity turn)
- AoA during second-stage flight
- AoA during descent

The following parameters were not varied:

- AoA during first stage flight: In order to reduce loads during the critical phase of maximum dynamic pressure, the AoA is nominally set to be 0° during first stage flight.
- Bank angle: As shown in chapter 3, the Starship does not have sufficient cross-range to curve around large populated areas. Thus, the nominal bank angle during descent was kept at 0°. In an actual mission, banking maneuvers could be used to correct insertion errors and precisely arrive at the designated landing area.

4.1.2.3 Optimization objectives For both systems, the minimization of the peak heat flux was an objective for the optimization. For the Starship, this was the sole objective while for the SpaceLiner mission the total overflown population was an additional minimization objective [12].

4.1.3 Optimization framework

The aforementioned constraints, controls, initial conditions, and vehicles properties were evaluated with the NSGA3 algorithm [13] [14] implemented within the Pymoo framework [15].

4.2 Results

The following sections contain the results of full mission evaluations, including the ascent of both stages as well as the descent of the orbital stage down to 10 km altitude. The subsequent subsonic final approach and landing are not modeled for either vehicle.

While the first section 4.2.1 focuses on a generic evaluation with a fixed range and variation of the travel direction, the second section focuses on a specific mission from California to Shanghai and back.

4.2.1 Effect of heading

For orbital transport systems, it is well established that the heading of the launch vehicle has a major impact on the performance due to the Earth's rotation. While the missions discussed herein are technically suborbital, the impact of the heading is still significant.

In Sect. 3.4, the effect during reentry was discussed. For identical initial relative velocities, the distance covered within the atmosphere is significantly less for both reference vehicles when flying westward. For a full mission however, the ascent and ballistic portion of the flight can compensate this range loss and still assure sufficient range is covered for successful completion of the mission. For either heading, the Starship has a lower range compared to the SLO, once the denser portion of the atmosphere is entered. This means that the Starship has to rely much more on the ballistic portion of the flight to cover the desired distance.

In order to reach an identical ballistic arch toward the west, compared to an eastward trajectory, Earth's rotational

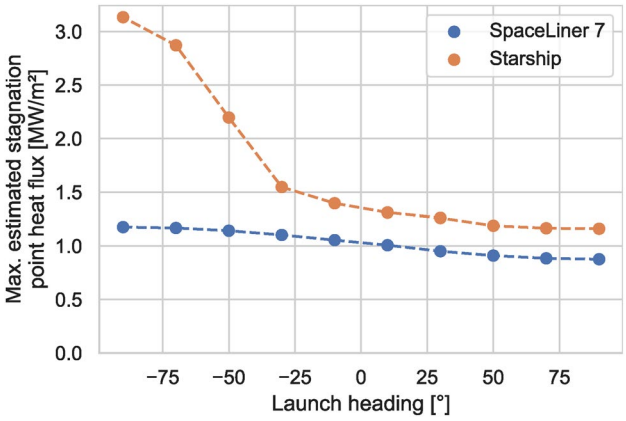

Fig. 9 Peak heat flux for a PTP mission with 10,000 km range for various launch headings. Heat flux is estimated for both systems with a nose radius of 20.5 cm

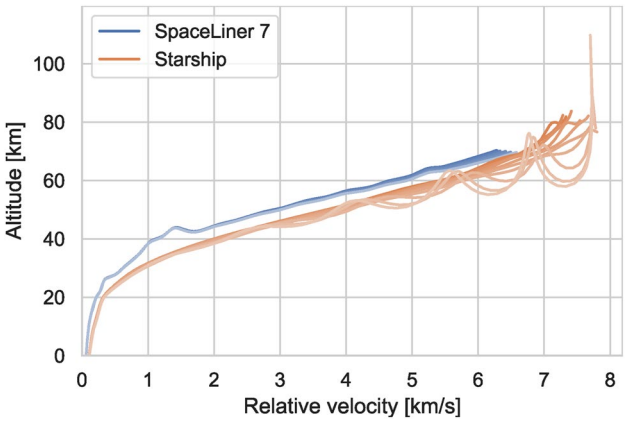

Fig. 10 Reentry profile for a generic mission with 10000 km range for various launch headings. Darkest shades are for eastward launch headings, lightest shades for due west

speed has to be compensated twofold by the stage. At the equator, this would mean over 900 m/s additionally required Δv. Alternatively, the ballistic range of the vehicle can also be increased by flying a steeper ascent with subsequently a higher apogee. However, this will inexorably lead to a steeper reentry and thus higher peak heat fluxes. The trajectory optimizer has to identify a compromise between these two approaches to compensate the westward range loss. Both options inherently lead to higher heat fluxes, one by resulting in a higher initial relative velocity and the other in a steeper reentry. For both vehicles, this means that routes in a westward direction will be more challenging with regard to the heat flux encountered and/or Δv budget necessary.

In order to quantify and illustrate this effect, the following parametric study was undertaken. For a variety of launch headings ranging from due east (90°) to due west (-90°), a trajectory was optimized for a 10,000 km travel distance and for minimal heat flux, assuming the reference payload from Table 1. The resulting maximum heat fluxes are shown in Fig. 9. To understand the different behavior of both systems, the reentry profile has to be evaluated too (illustrated in Fig. 10).

Some interesting observations can be made here: First, the 10,000 km range mission necessitates higher separation velocities for the Starship system, due to its reliance on the ballistic portion of the trajectory to cover the distance. It is also apparent, that for the eastward mission, both the Starship and SpaceLiner system did not need to use their maximum Δv budget. With the launch direction changing to more westward headings, the optimized separation velocity increases for both systems. This is in line with expectations, since the vehicle has to compensate for the rotational velocity of the Earth, as mentioned previously.

It should also be noted that even though the Starship relies on the ballistic portion of its flight to cover the majority of the distance, the resulting trajectory is still very shallow in order to reduce the peak heat fluxes.

Heading eastwards, all trajectories generally follow the same pattern, with the trajectory staying shallow, albeit with rising SECO velocities for lower launch headings. As can be seen in Fig. 9, this already leads to slightly increased peak heat fluxes. For launch headings smaller than -30°, the second-stage operation time upper boundary is reached for the Starship. In these cases, the only option for the optimizer to fulfill the mission is to fly higher ballistic arches which lead to significantly higher peak heat fluxes, resulting in the values shown in Fig. 9. The increase in maximum altitude can also be seen in the reentry profile as well as the skipping, which results from the steeper initial reentry.

The SpaceLiner system does not exhibit the same behavior. While the SECO velocity also increases for launch headings toward the west, the gliding range is always sufficient to achieve the mission without having to resort to higher ballistic arches and the subsequent increase in peak heat flux.

It shall be noted, that the maximum permissible heat load for the Starship stage is not known, as is the point at which the heat flux might have a significant impact on the refurbishment cost or turnaround time. It is therefore likely but not certain that this effect will impact the selection of feasible routes, or the payload that can be delivered in each direction. This effect will likely become more pronounced with increasing range demands.

It shall also be noted that the results and discussions in this section focused on an equatorial launch. The effect of launch heading can be expected to vary with changing latitudes, with the velocity caused by Earth's rotation being smaller at higher latitudes and the effect is expected to disappear for a theoretical launch site at either of the poles.

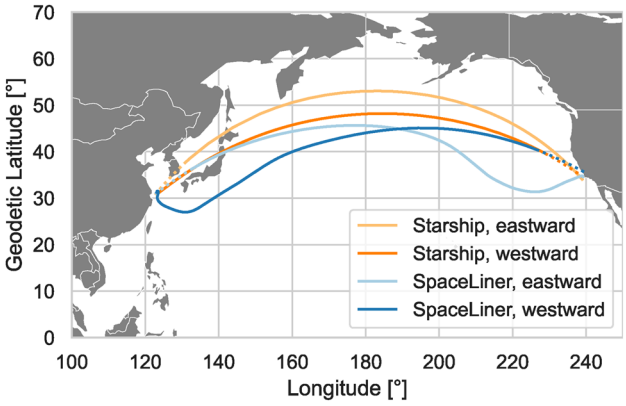

Fig. 11 PTP trajectories for Starship and SpaceLiner Orbiter between Shanghai and California

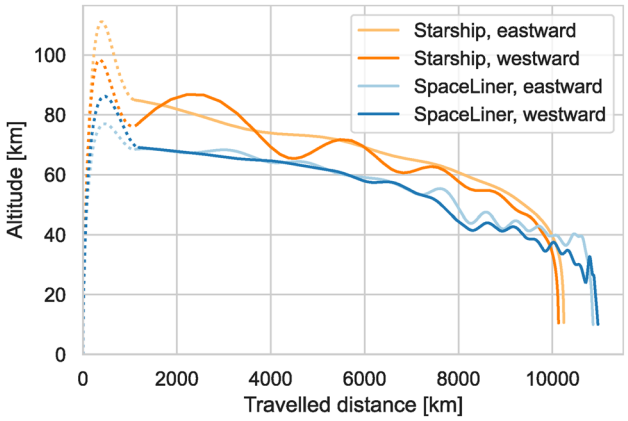

Fig. 12 Altitude over downrange for PTP mission of Starship and SpaceLiner

4.2.2 Point-to-point mission between Shanghai and California

For the final comparison, two specific PTP missions were evaluated for the Starship and SpaceLiner systems: from Shanghai to California and the return flight. The flight paths for both reference systems are shown in Fig. 11. In all following figures, the ascent is shown as a dotted line and the descent as a continuous line.

As noted in section 4.1, the trajectory optimization for the SpaceLiner includes the overflown population density as a minimization objective. The effect is clearly visible: Instead of following the great circle of minimum distance, the SpaceLiner trajectories head further southward and perform a banking maneuver in order to approach the final target without passing close to the highly populated coastal areas. As the Starship trajectory optimization does not include this constraint, the flight path takes the Starship directly to the target coordinates. As shown in chapter 3, the crossrange ability by banking is limited for the Starship, thus no banking in order to avoid populated areas was considered. In future studies, the option of actively changing the heading through propulsive maneuvers and thus gaining the ability to dogleg around population centers could be of interest. This option would however seriously increase the Δv requirements of the mission. Another option is the avoidance of populated areas by increasing the altitude, which would at least reduce or eliminate the sonic boom impact.

The altitude profile over the traveled distance for both vehicles is shown in Fig. 12.

For both vehicles, the highest altitudes are achieved during the ascent. The Starship trajectories are generally higher than the equivalent SpaceLiner trajectories, needing to find a compromise between avoiding the drag of the upper atmosphere and while still enabling a shallow reentry when the denser layers of the atmosphere are finally entered. The higher altitude also mitigates the sonic boom impact while overflying populations.

Looking at the trajectory profile over time (see Fig. 13), it becomes apparent that the Starship mission is noticeably faster than the same mission for the SpaceLiner. This is caused by three effects:

A) Starship descent starts at higher velocities,
B) The curved SpaceLiner trajectory leads to longer distances traveled,
C) The two vehicles have different deceleration profiles.

While the Starship flies at near-orbital velocities for almost the entire mission and then decelerates rapidly, the SpaceLiner has an almost constant deceleration throughout the mission, as can be seen in. Fig. 14. While this leads to similar mean velocities when averaging over time, the

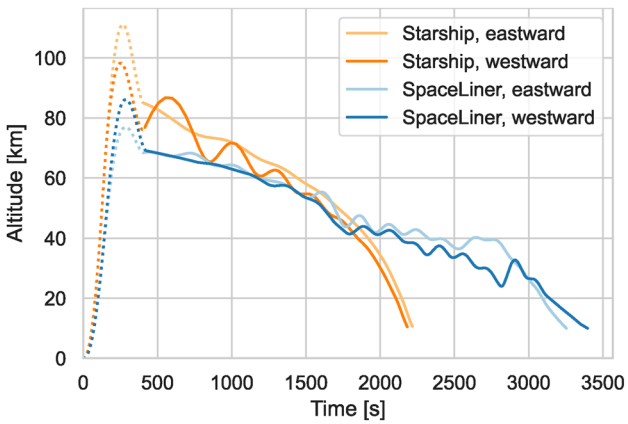

Fig. 13 Altitude over time for PTP mission of Starship and SpaceLiner

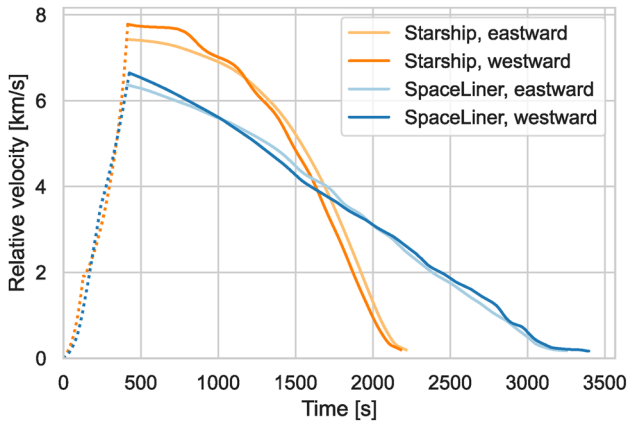

Fig. 14 Relative velocity over time for PTP missions of Starship and SpaceLiner

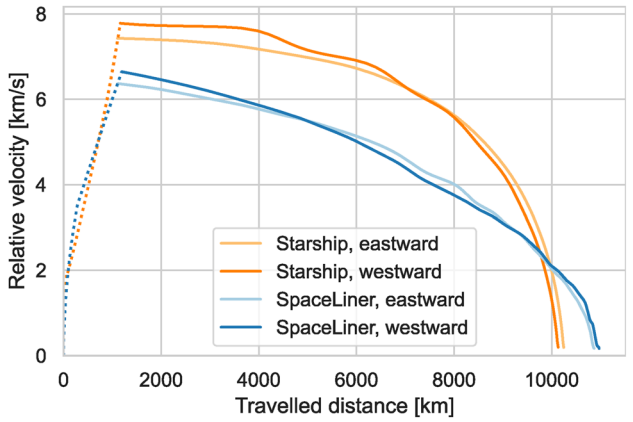

Fig. 15 Relative velocity over distance traveled for PTP mission of Starship and SpaceLiner

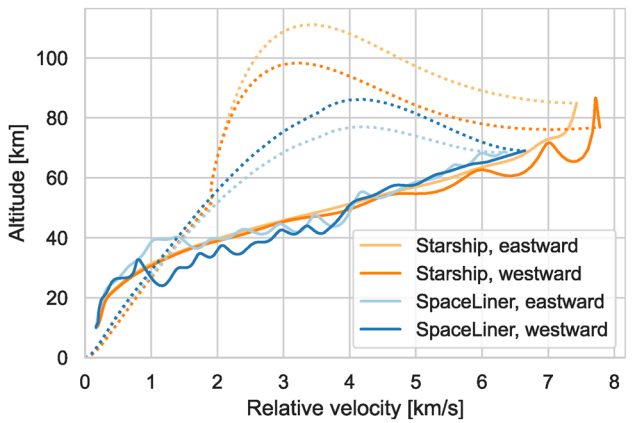

Fig. 16 Reentry profile for PTP mission of Starship and SpaceLiner

relevant average over the distance is significantly different as shown in Fig. 15.

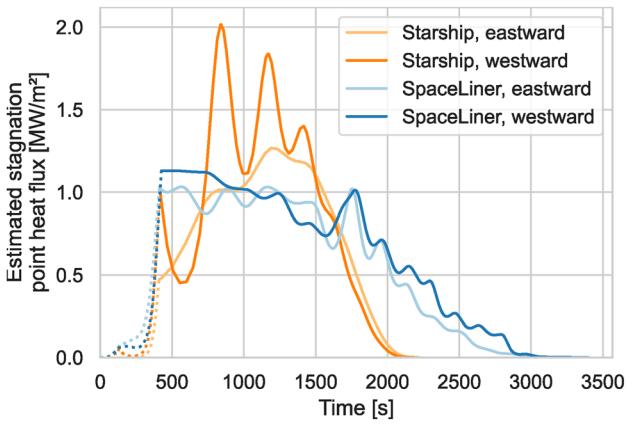

Fig. 17 Heat flux over time for PTP mission of Starship and SpaceLiner. Stagnation point heat flux is estimated for both systems with a nose radius of 20.5 cm

The large difference in maximum relative velocity is also apparent in the reentry profile, shown in Fig. 16. In order to cover the same distance, the Starship is accelerated to much higher SECO velocities. The SpaceLiner can achieve the same mission with a lower SECO velocity due to the much higher hypersonic L/D ratio and its ability for prolonged atmospheric flight. In contrast, the Starship relies on a shallow ballistic arch to cover almost the entire distance. Initially, the SpaceLiner also flies in a quasi-ballistic manner, but it can extend that distance significantly in quasi-stationary hypersonic glide. For illustration, when looking at Fig. 12 and specifically the remaining distance that is covered after descending to 60 km, it can be seen that the Starship mission only flies for another 2000 km while the SpaceLiner still covers over 5000 km. This difference has an especially large impact when launching toward a westward trajectory.

As can be seen in Fig. 16, both vehicles accelerate to higher velocities for the westward mission, than for the eastward mission. This effect and its cause, the Earth's rotational velocity, have been discussed in section 4.2.1. In this case, the effect is compensated by higher relative velocities. Due to the higher reliance on the ballistic portion of the trajectory to cover distances, the difference between the relative velocities is higher for the Starship mission.

In general, the reentry profile for both vehicles is alike since both vehicles need to avoid the denser parts of the atmosphere until sufficiently decelerated. While both SpaceLiner missions have a very similar reentry profile, for the Starship missions, some differences are visible. It can be seen that for the westward trajectory, the Starship dips deeper into the atmosphere. The effect of this, higher heat fluxes, is shown in Fig. 17.

Both transport systems are able to achieve their missions, albeit with the aforementioned increased heat fluxes for the

Starship system for the westward mission. However, this might be mitigated by reduction of the payload mass, which was set to 100t for this comparison.

In both cases, the acceleration experienced by the passengers is deemed acceptable, with the maximum acceleration during the reentry being less than 1.4 g for the Starship and 2.1 g for the SpaceLiner. The higher value for the SpaceLiner is caused by the banking maneuvers close to the landing area for the westward trajectory. For the eastward trajectory, the maximum acceleration is 1.5 g. The altitude oscillations visible in parts of the SpaceLiner's trajectories will likely not impact the passenger comfort since the period is fairly large (~ 2.5 min). Additionally, as described in Sect. 4.1, the trajectory was not optimized in order to reduce these oscillations. Further numerical effort could be used to reduce them. However, this local refinement of the controls is expected to only have a minor effect on the vehicle's performance.

5 Conclusion and outlook

Potential PTP missions were evaluated for two reference vehicles, the SpaceLiner 7 and the Starship system. From a system perspective, the major differences are the choice of propellant and recovery/reentry methods for the stages. While the Starship is designed with the low dry mass options LOX/LCH4 and vertical landing for recovery of the stages, the SpaceLiner system is designed with LOX/LH2 and winged horizontal reentry and landing. This leads to a system with overall higher structural indexes, but higher specific impulse and lower Δv requirement for the same PTP mission.

While the Starship is designed for a fast deceleration once it enters the atmosphere, the SLO can cover significant distances in a quasi-stationary glide flight. This leads to a higher dependency of the Starship on the ballistic portion of the trajectory which results in higher Δv requirements, especially for missions contrary to the Earth's rotation.

From a technical/physical perspective, both systems appear able to perform these types of missions. Due to their very different reentry types, they do exhibit individual strengths and weaknesses but show no general showstoppers.

The economic feasibility of such transport systems will be highly dependent on the recurring costs and the number of flights actually undertaken. While both systems aim for low recurring cost, the reality of the refurbishment need is currently unknown and will likely only be known once the vehicles are actually operational. This might soon be the case for SpaceX's Starship system, but as a private company, they might not share that information with the public.

All the missions analyzed in chapter 4 targeted a similar range, close to 10,000 km. In future evaluations, longer missions should also be evaluated, to see if the trends shown here hold for the ultra-long-distance as well. The time benefit of these rocket-propelled systems compared to conventional airliners increases with increasing travel distances so the longer distance missions are of special interest.

While the small number of current rocket launches have small impact on the atmosphere, with rising launch cadences, the impact of such systems on the Earth's climate should be analyzed and considered in future studies.

Funding Open Access funding enabled and organized by Projekt DEAL. Part of this work was performed within the project 'European Concept of Higher Airspace Operations' (ECHO). This project has received funding from the SESAR Joint Undertaking (JU) under grant agreement No 890417. The JU receives support from the European Union's Horizon 2020 research and innovation program and the SESAR JU members other than the Union. Further information on ECHO can be found at https://higherairspace.eu/

Declarations

Conflicts of interest The authors have no relevant financial or non-financial interests to disclose.

References

1. SpaceX, SpaceX - Starship, [Online]. Available: https://www.spacex.com/vehicles/starship/. Accessed 08 2022.
2. SpaceX, "SpaceX - Missions: Earth," [Online]. Available: https://www.spacex.com/human-spaceflight/earth/index.html. Accessed 08 2022.
3. M. Sippel, J. Klevanski and J. Steelant, , 2005 Comparative Study on Options for High Speed Intercontinental Passenger Transports, in 56th International Astronautical Conference 2005.
4. Sippel, M., Trivailo, O., Bussler, L., Lipp, S., Valluchi, C.: Evolution of the SpaceLiner towards a Reusable TSTO-Launcher, in International Astronautical Congress. Guadalajara, Mexico (2016)
5. J. Wilken, M. Sippel and M. Berger, 2022 Critical Analysis of SpaceX's Next Generation Space Transportation, in 2nd International Conference on High-Speed Vehicle Science Technology (HiSST). Bruges. Belgium.
6. SpaceX, 2016 Making Life Multiplanetary. [Online]. Available: https://www.spacex.com/media/making_life_multiplanetary_2016.pdf. Accessed 08 2022.

7. Sippel, M., Stappert, S., Koch, A.D.: "Assessment of Multiple Mission Reuasble Launch Vehicles," in *69th International Astronautical Congress*. Bremen, Germany (2018)
8. M. Sippel, S. Stappert, Y. M. Bayrak, L. Bussler and S. Callsen, 2022 Systematic Assessment of SpaceLiner Passenger Cabin Emergency Seperation Using Multi-Body Simulations, in 2nd International Conference on High-Speed Vehicle Science Technology. Bruges. Belgium.
9. M. Sippel, S. Stappert and S. Singh, 2022. RLV-Return Mode In-Air-Capturing and Definition of its Development Roadmap, in 9th European Conference for Aeronautics and Space Sciences (EUCASS) 2022, Lille, France
10. Van Foreest, A., Sippel, M., Gülhan, A., Esser, B., Ambrosius, B.A.C., Sudmeijer, K.: Transpiration cooling using liquid water. J Thermophys. Heat. Trans. **23**, 693 (2009)
11. T. Dodd, "Go up SpaceX's Starship-catching robotic launch tower with Elon Musk!. 26 05 2022. [Online]. Available: https://youtu.be/XP5k3ZzPf_0. Accessed 09 2022.
12. Callsen, S., Wilken, J., Sippel, M.: "Feasible options for point-to-point passenger transport with rocket propelled reusable launch vehicles," in *73rd International Astronautical Congress (IAC)*. France, Paris (2022)
13. Deb, K., Jain, H.: An evolutionary many-objective optimization algorithm using reference-point-based nondominated sorting approach, part I: solving problems with box constraints. IEEE Trans. Evol. Comput. **18**, 577–601 (2014)
14. Jain, H., Deb, K.: An evolutionary many-objective optimization algorithm using reference-point based nondominated sorting approach, part II: handling constraints and extending to an adaptive approach. IEEE Trans. Evol. Comput. **18**, 602–622 (2014)
15. Blank, J., Deb, K.: Pymoo: multi-objective optimization in python. IEEEAccess. **8**, 89487 (2020)